"Spin Transport and Spin Thermoelectric Transport in 2D Mn-Doped Blue Phosphorene with High Curie Temperature and Half-Metallicity"

Xuming Wu,[†] Lei Hu,[†] Dandan Gu,[†] and Guoying Gao [*,†,‡],

[†] School of Physics, Huazhong University of Science and Technology, Wuhan 430074, China

[‡] Wuhan National High Magnetic Field Center, Huazhong University of Science and Technology, Wuhan 430074, China
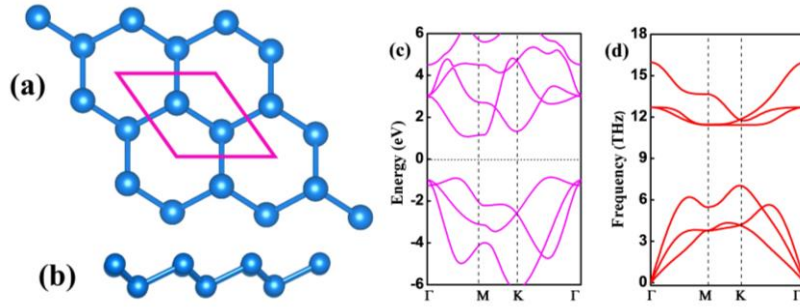
*guoying_gao@mail.hust.edu.cn

Figure S1. The top view (a), side view (b), band structure (c), and phonon spectrum (d) of monolayer blue phosphorene.
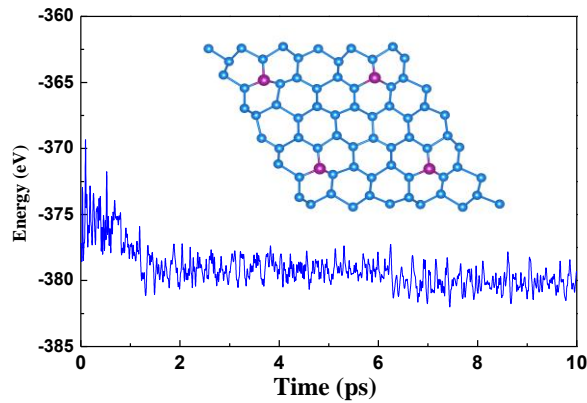

Figure S2. The total potential energy fluctuation of the 6×6×1 supercell for Mn-doped monolayer blue phosphorene during the AIMD simulations at 400 K. The inset is the structure of Mn-doped monolayer blue phosphorene at the end of 10 ps in the AIMD simulations.
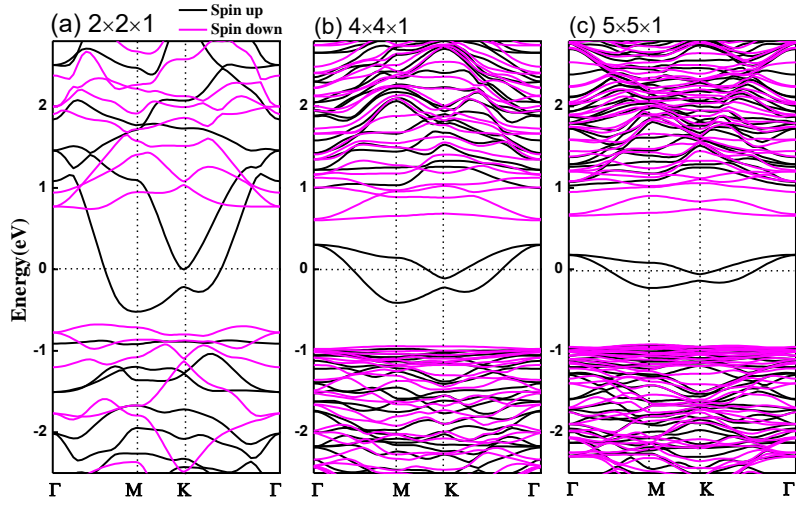
Figure S3. The calculated spin-dependent band structures within GGA-PBE for the Mn-doped monolayer blue phosphorene with the impurity concentration of 12.5%, 3.1% and 2% based on the 2×2×1, 4×4×1 and 5×5×1 supercells, respectively.
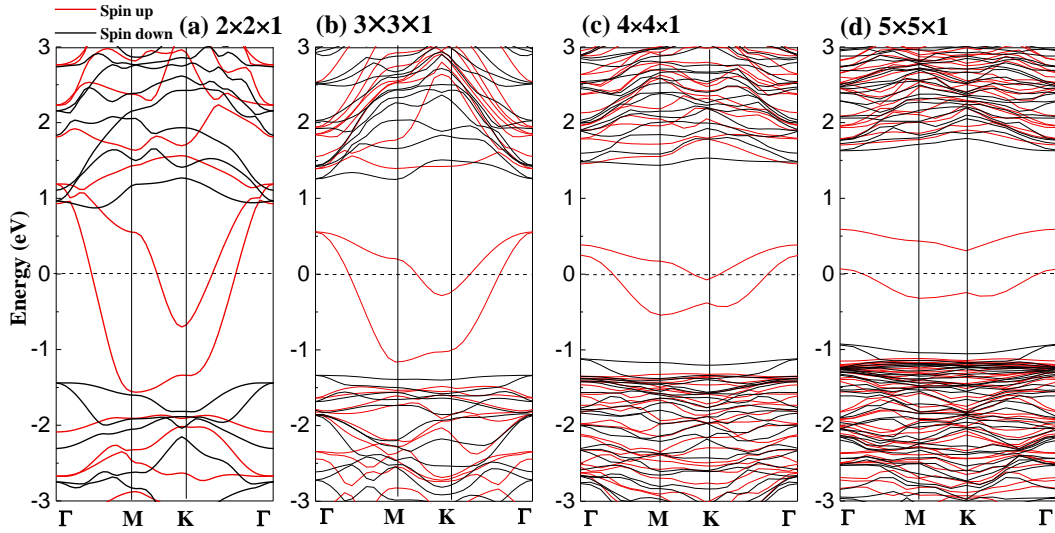

Figure S4. The spin-dependent band structures within HSE06 for the Mn-doped monolayer blue phosphorene with the impurity concentration of 12.5%, 5.56%, 3.1% and 2% based on the 2×2×1, 3×3×1, 4×4×1 and 5×5×1 supercells, respectively.
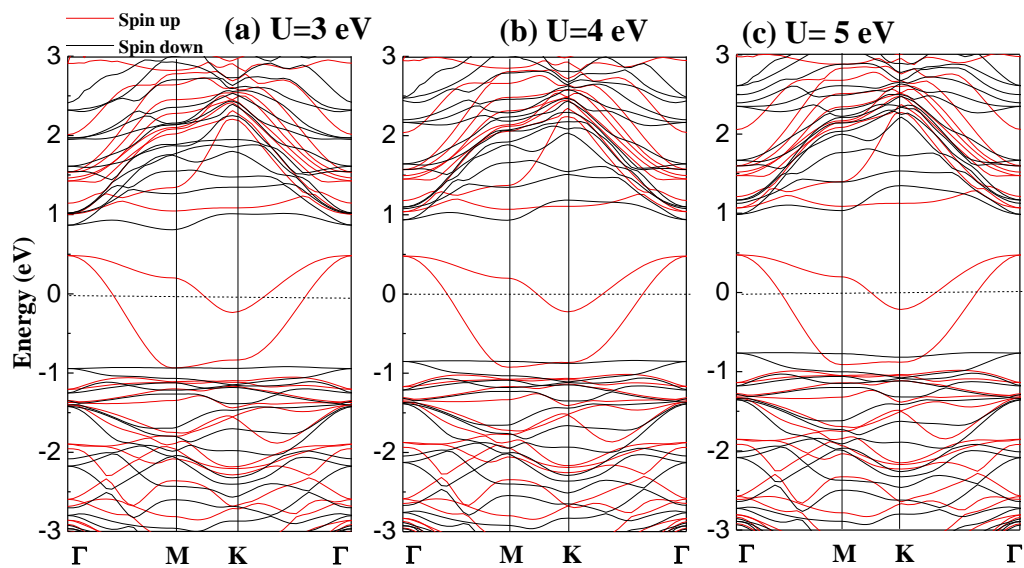
Figure S5. The spin-dependent band structures within PBE+U (U=3 eV (a), 4 eV (b) and 5 eV (c)) for the 5.56% Mn-doped monolayer blue phosphorene based on the $3\times3\times1$ supercell.
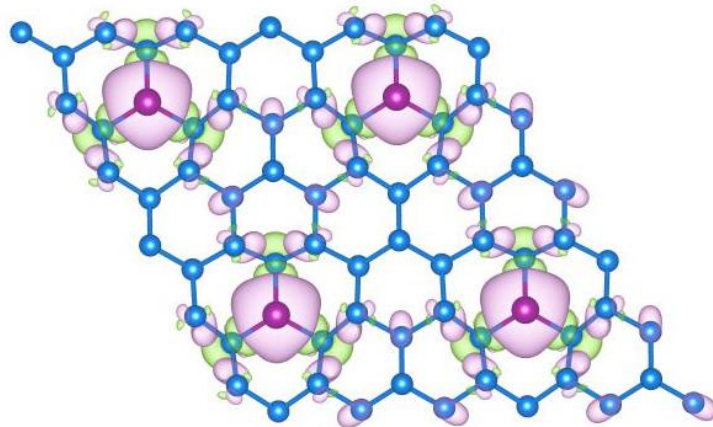

Figure S6. Spin density of Mn-doped monolayer blue phosphorene. Purple and cyan isosurfaces represent the positive and negative spin densities (0.00674 e/$Å^3$), respectively.
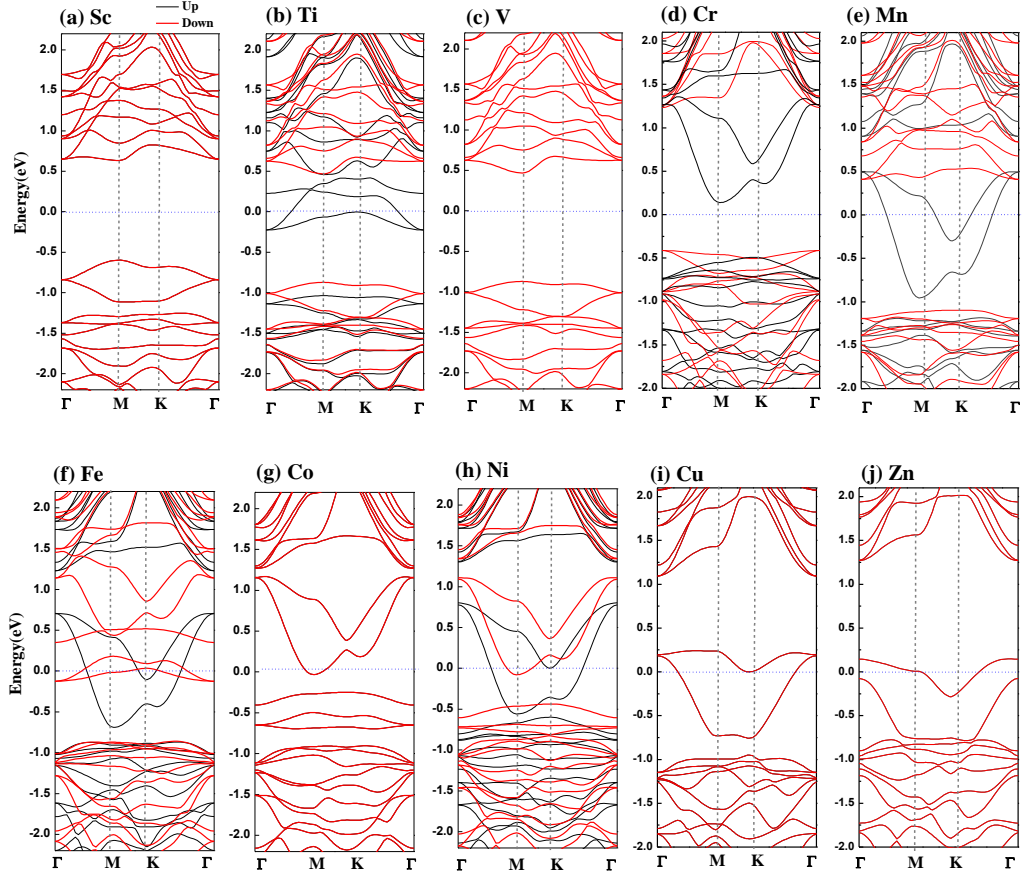
Figure S7. The spin-dependent band structures within GGA-PBE for the monolayer blue phosphorene doped with different transition metals based on the 3×3×1 supercell.